International Research Journal on Advanced Engineering and Management
https://goldncloudpublications.com
https://doi.org/10.47392/IRJAEM.2024.0263
e ISSN: 2584-2854
Volume: 02
Issue: 05 May 2024
Page No: 1771-1777

Design of Resonant Converter of Trans-Cutaneous Energy Transfer System to Power Artificial Heart

Sarath S Nair[1], *Harikrishnan S*[2]
[1] *Scientist/Engineer F, Department of Medical Devices Engineering, Biomedical Technology Wing, SCTIMST, Thiruvananthapuram, Kerala, India.*
[2] *Professor, Department of Cardiology, SCTIMST, Thiruvananthapuram, Kerala, India.*
Email Id: *saraths@sctimst.ac.in*[1], *drhari@sctimst.ac.in*[2]

Abstract
Wireless technologies have matured to recharge the batteries of consumer devices efficiently. The benefit of the technology is being used by mobile communication devices, personal computation devices, and wearable entertainment devices. The wireless energy transfer techniques employ the transfer of electrical energy between two-tesla coils in surface contact and not by electrical contact through the phenomenon of electromagnetic induction. Many international consortiums have made guidelines for designing and manufacturing these devices. However, for active implantable medical devices such as artificial hearts, a large amount of electrical energy usually in the range of 15W to 30W needs to be transferred across the skin at a depth of 10mm to 30mm. The design needs to be optimized for maximum power transfer with the highest possible efficiency. Any loss in power will be reflected as heat energy and cause burns and tissue death. A transcutaneous energy transfer system is such type of wireless energy transfer mechanism across the skin to power implanted life-saving devices. In this paper, the design of a resonant converter and its performance is investigated to wirelessly transfer electrical power up to a tissue thickness of about 25mm.
Keywords: *Artificial heart, Transcutaneous Power Transfer, Wireless Energy Transfer, Resonant Converters.*

1. Introduction

A transcutaneous energy transfer system transmits electrical power across the skin which consists of a primary side transmitter circuitry that is kept over the skin and a secondary side receiver circuitry kept subcutaneously under the tissue within the body [1,2,3]. The primary side transmitter circuitry consists of a spiral wound pancake coil, a resonating capacitor, and a full bridge resonant circuit. The spiral wound coil is connected in series with the resonating capacitor which in turn is connected to the resonant full bridge converter. The secondary side receiver circuitry of the system consists of a series connected spiral wound pancake type receiving coil and a resonant capacitor connected to a full bridge resonant bridge rectifier. The output of the rectifier is filtered using a capacitor and connected to the active implantable medical devices such as artificial hearts [4,7,8]. The overall efficiency of the system is the product of the efficiency of the individual subsystems. Since all the subsystems are attached to the body, sub-optimal operation of any of the components leads to high thermal dissipation leading to localized temperature rise and subsequent health hazards. Hence every effort must be taken to ensure the optimal design of the system. Much research has happened in the last few decades to create the most efficient mechanism for delivering power to implanted devices [5,11,12,14,15,16]. Resonant high-frequency converters are found to be the best choice due to their high operating efficiency and easiness of control [6,9,10,]. However, the practical implementation of the TETS system to the clinical scenario is very limited too few experiments [17,18] Unlike commercial available wireless power transfer systems, TETS shall operate in an efficient manner at varying axial gap. The thickness of the skin can vary between 5mm to 25 mm depending on the fat deposit of the patient. More over the design should be reliable,

International Research Journal on Advanced Engineering and Management
https://goldncloudpublications.com
https://doi.org/10.47392/IRJAEM.2024.0263
e ISSN: 2584-2854
Volume: 02
Issue: 05 May 2024
Page No: 1771-1777

robust and less foot print hardware configuration suitable for implantable medical application. The entire hardware system should be handy, less weight and made of biocompatible materials. Robustness of design is of utmost importance. The number of components shall be minimum. The system should have adjustable power for various medical requirements, and life time operation. Considering these requirements, the design of a resonant converter to deliver power up to 20W at a distance of 25mm is provided in this paper. A schematic circuit of the same as well as the hardware development is provided. The performance of the converter is studied to understand the power transfer capability, voltage gain, and efficiency. Session 2 describes the Methods employed for overall system fabrication, coil fabrication, primary side and secondary side hardware fabrication. Session 3 describes the circuit verification, and the performance evaluation for different load conditions and axial gap conditions.

2. Method

2.1. Overall System

As shown in Figure 1, the transcutaneous energy transfer system consists of an externally kept primary side subsystem and an implanted secondary side subsystem which are tuned to the same resonant frequency [9]. The primary side subsystem consists of a DC source connected to a high-frequency power inverter and a spiral-wound pancake coil. The secondary side subsystem consists of a coil electrically connected to a high-frequency rectifier, which in turn is connected to the load.

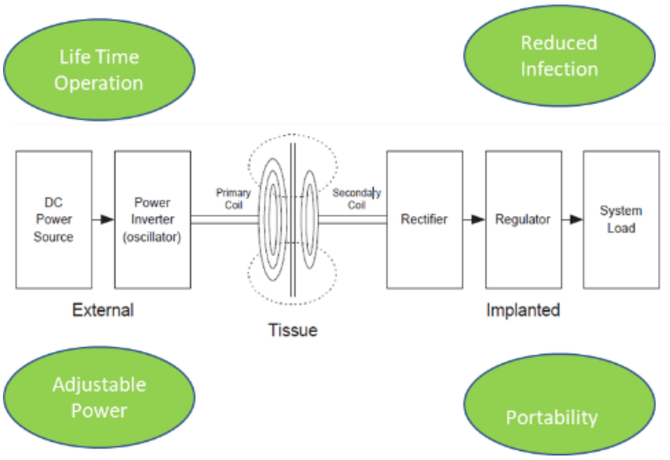

Figure 1 TETS Architecture

The primary side and the secondary side subsystems are magnetically coupled through the skin and tissues. As for any resonant circuits, maximum power can be transferred by operating the system at its resonant frequency. A practical combination of coil inductance and capacitance values shall be taken to achieve a realizable system [18]. In this case, to operate the system at a resonant frequency of 150kHz, a coil with an inductance value of 40uH connected to a capacitance of 27nF is selected for the primary side. Similarly, the coil in the secondary side has an inductance of 40uH and is connected to a 27NF capacitor to establish resonance thus enabling maximum power transfer. The series combination of a secondary coil and a capacitor is connected to a full wave bridge rectifier followed by a capacitive filter for removing the ripples.

2.2. Power Transfer Coil

To implement a practical TETS system, a planar spiral coil configuration is selected [13]. The specifications such as diameter, wire diameter, and wire spacing are designed as the modified Harold Wheeler approximations provided in [10]. To obtain the primary and secondary coil as per the design process, the spiral coil is made by winding, 35 turns of 0.7mm diameter, 300 strands SWG 44 Litz wire into a diameter of 70mm. The planar coil is impregnated with 1mm thick epoxy for obtaining structural rigidity as shown in Figure 2. The leads of the coils are cleaned and removed for the enamel coating for measurement and soldering to the control board.

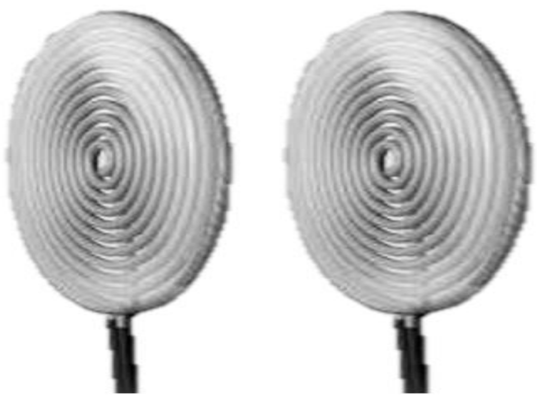

Figure 2 TETS Coils

International Research Journal on Advanced Engineering and Management
https://goldncloudpublications.com
https://doi.org/10.47392/IRJAEM.2024.0263
e ISSN: 2584-2854
Volume: 02
Issue: 05 May 2024
Page No: 1771-1777

2.3. Primary Side Full Bridge Resonant Inverter

Considering the various merits in comparison with other topologies as detailed in [6,9,10], a resonant full wave H bridge circuit is considered for TETS hardware implementation The primary side full bridge resonant inverter circuit for the system is designed using Proteus electronic CAD software shown in Figure 3. The circuit consists of an H bridge combination of four numbers of low resistance MOSFET in parallel to a snubber circuit as shown in Figure 3. The primary coil is connected to the midpoints of the H bridge circuit. To have the best results, the full wave resonant inverter is made of MOSFET p55nF06 having an R_{dson} of 18mohms. The MOSFET is selected based on the least resistance it offers while conduction. The MOSFETs are turned on and off using a frequency-controlled gate drive circuitry. The gate drive circuit consists of a frequency generator, and two dual high-low-side MOSFET driver IR2110. The frequency of the gate drive circuitry can be varied by adjusting a resistor value to obtain frequencies in the range of 50kHz to 500kHz. The full wave inverter is fed with a constant source of 15V or 24V DC. When powered on, the pulse generator provides the frequency based on the program run in the microcontroller.

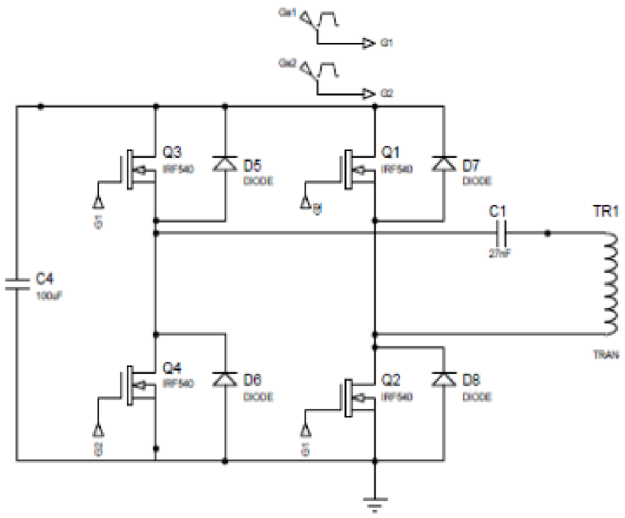

Figure 3 **Primary Side Resonant Inverter**

The pulse is provided to two IR2110 which in turn is connected to the high and low side MOSFET in each leg of the H bridge. The IR2110 has a bootstrap configuration to produce a high voltage to turn on the upper MOSFETs. The gate drive circuitry turns on the MOSFETs such that, the DC voltage is converted into a sinusoidal voltage of a said frequency. To protect the MOSFETs from failures, an RC snubber circuit consisting of a 10M resistor in series with a 600pF capacitor is connected in parallel to each MOSFET. The primary coil in series with a 27nF ceramic capacitor is connected to the middle pints of the H bridge. Figure 4 shows the schematics of the entire circuit consisting of the H bridge inverter, pulse generator, and MoSFET drivers. The schematics are converted to a Layout using Proteus Aries software. The layout is made to a small footprint SMD package components suitable for over-the-skin placement as shown in Figure 5.

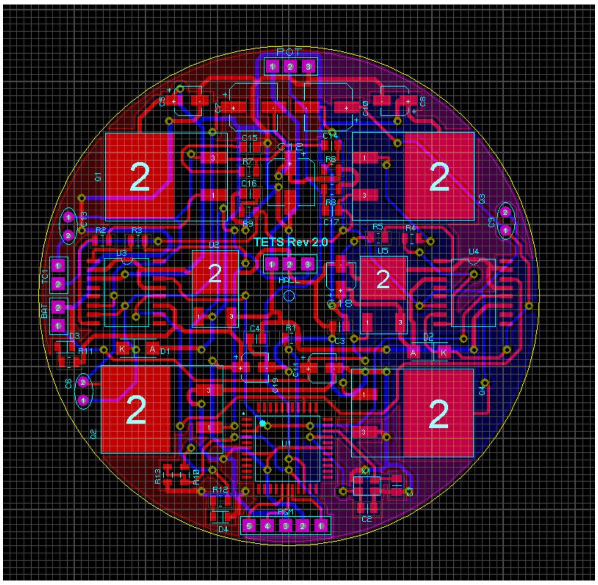

Figure 4 **PCB Layout of the Primary Side Resonant Circuit**

2.4. Secondary Side High Frequency Rectifier

The secondary coil is connected to a full wave bridge rectifier followed by a capacitive filter for removing the ripples. The rectifier consists of four numbers of high-frequency Schottky diodes kept in an H bridge combination. A variable load resistance in the range of 10 to 40 ohms which mimics the actual medical device load is connected

International Research Journal on Advanced Engineering and Management
https://goldncloudpublications.com
https://doi.org/10.47392/IRJAEM.2024.0263
e ISSN: 2584-2854
Volume: 02
Issue: 05 May 2024
Page No: 1771-1777

across the filter capacitor. When powered on, voltage is induced on the secondary coil due to electromagnetic induction, and power is transferred from the primary coil to the secondary coil. The resistance of the gate drive circuitry is adjusted to obtain the performance of the system under variable frequency and to understand its characteristics such as voltage gain, current power drawn, and efficiency. The layout of the printed circuit board is designed in PROTEUS ARES software as shown in Figure 5.

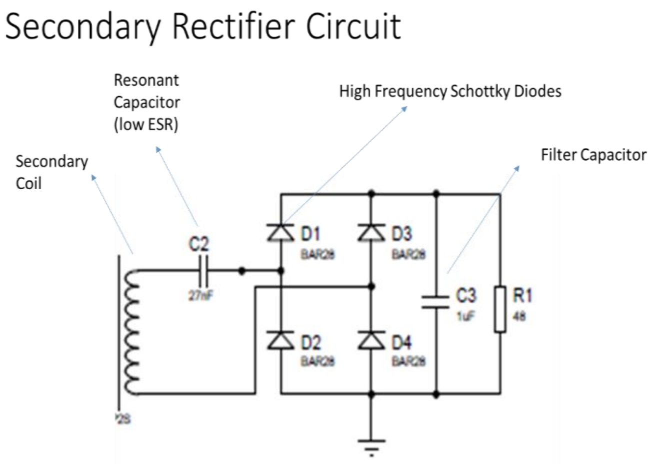

Figure 5 **Secondary Side High Frequency Rectified Circuit**

3. Results And Discussion

The system as described above is fabricated into a PCB as shown in Figure 6. When the primary side transmitter circuit is powered by a battery or a suitable direct current source, the full bridge resonant circuit generates a high-frequency square wave pulse to pass through the series-connected spiral coil and resonant capacitor. The combination of the spiral coil and the capacitor produces a sinusoidal voltage across the spiral coil inductor when exited with the square wave input as shown in Figure 9(Yellow colored). The magnitude of the sinusoidal voltage varies with the frequency and becomes maximum at a characteristic frequency called resonant frequency, which in turn is a parameter depending on the inductance of the transmitting spiral coil, primary side capacitor, and the coefficient of coupling between the primary side transmitting coil and the secondary side receiving coil. The sinusoidal voltage in the transmitting spiral coil produces an alternating electromagnetic field around the primary side coil. The electromagnetic field interacts with the secondary side receiving coil and induces a voltage in it due to Faraday's laws of electromagnetic induction as shown in Figure 7 (blue coloured). The generation of the voltage across the secondary side spiral coil is made to resonate with the presence of a capacitor connected in series with the secondary coil. At resonance, maximum energy is transferred from the primary side to the secondary side. The alternating voltage produced across the series is connected secondary side spiral coil and the capacitor is fed to the full bridge rectifier, which in turn converts it to a direct voltage as shown in Figure 7 (pink coloured). The direct voltage is then filtered to remove all ripples and provided to charge the battery and directly power the implanted artificial heart.

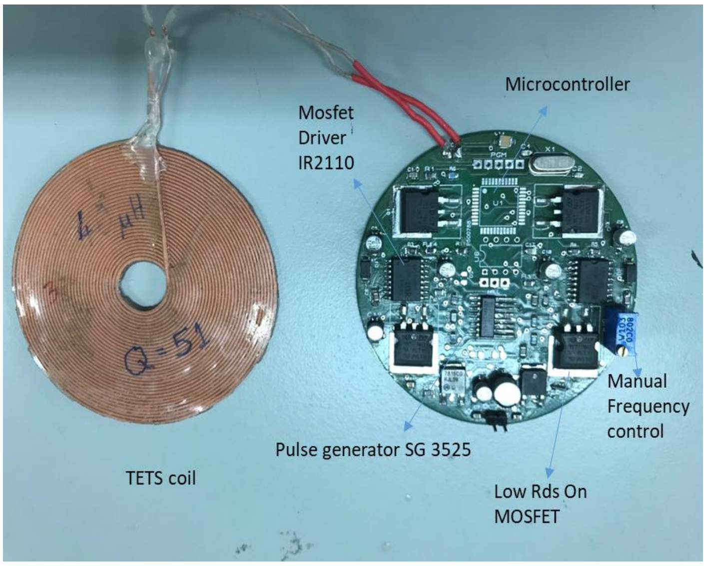

Figure 6 **Hardware of TETS System**

To study the performance, a variable load resistance in the range of 10 to 40 ohms which mimics the various medical devices is connected across the filter capacitor for understanding the performance. When powered on, voltage is induced on the secondary coil due to electromagnetic induction, and power is transferred from the primary coil to the secondary coil. The TETS system is tested on various resistive loads to understand the power output, efficiency, and voltage gain. As shown in Figure 8, an output power

International Research Journal on Advanced Engineering and Management
https://goldncloudpublications.com
https://doi.org/10.47392/IRJAEM.2024.0263
e ISSN: 2584-2854
Volume: 02
Issue: 05 May 2024
Page No: 1771-1777

of up to 20W can be produced by the system. The output power decreases when the load resistance decreases. A maximum efficiency of 60+/-5% is obtained for the load resistance of 20 ohms and 30 ohms. The efficiency decreased to less than 30% at a load resistance of 10 ohms. The voltage gain expresses the ratio of the output voltage to the input voltage given to the circuit in Figure 10.

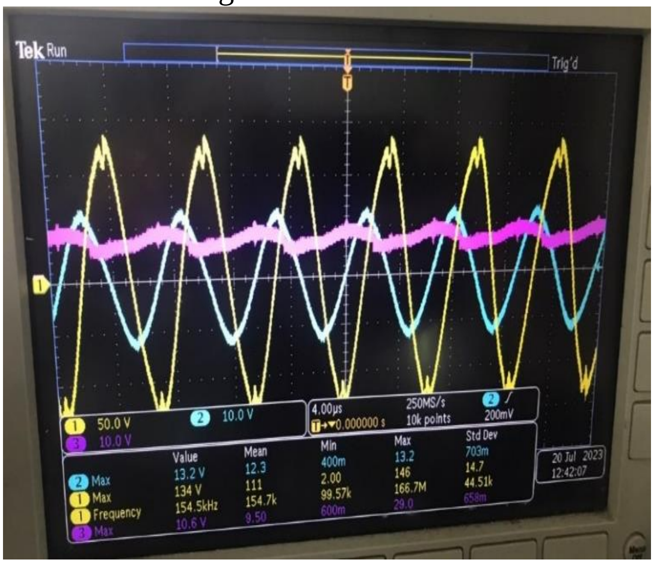

Figure 7 Voltages at Different Points of The TET System

As seen in Figure 10, the voltage gains increase with load resistance. At resistance below 20 ohms, the voltage gain is less than 1.0, whereas for the load resistance above 20 ohms, the voltage gain is above 1.0.

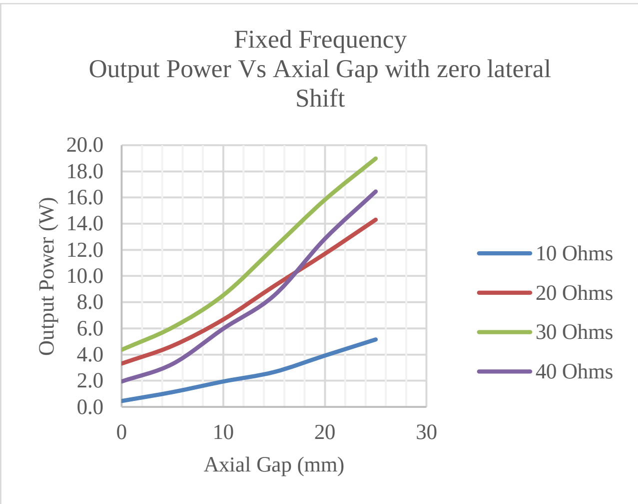

Figure 8 Output Power Produced

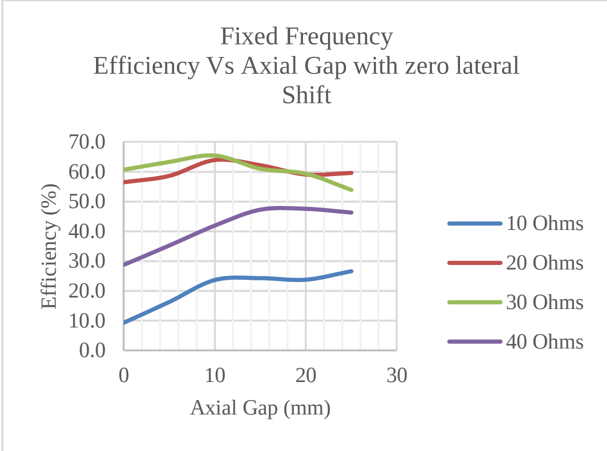

Figure 9 Output Power Produced

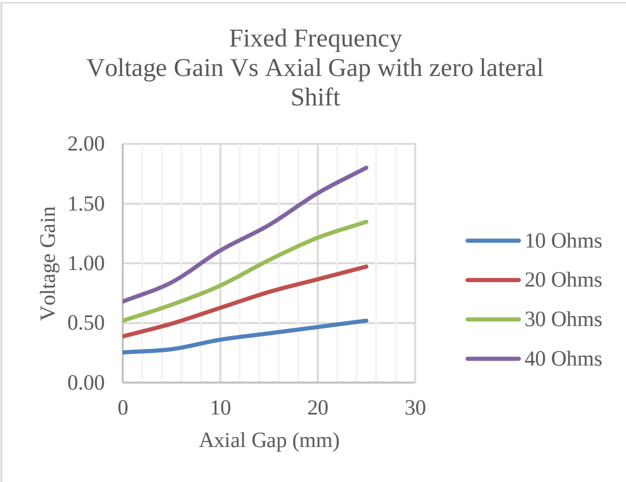

Figure 10 Output Power Produced

Conclusion

In this paper, the design of a resonant converter and its performance are investigated to wirelessly transfer electrical power up to a tissue thickness of about 25mm. The TETS system has been split into two subsystems namely, the primary side high-frequency inverter subsystem and the secondary side high-frequency rectifier subsystem. Two numbers of planar spiral coils in the shape of a pancake is made with 300 strands of SWG 44 Litz wire. The wire diameter of the Litz wire is 0.7mm and the overall diameter of the coil was 70mm. The primary coil circuit schematics and the secondary coil circuit schematics were prepared in Proteus ISIS software and a PCB is fabricated. The PCB with surface mount components are fabricated which is of small footprint to keep attached to the body. The system is operated at 150kHz with a 15V input DC supply to study the performance. It was noted that a maximum efficiency of 65% is obtained at a gap of 10 mm. Overall efficiency remains within 60+-5% for axial gaps in the range of 0 to 25mm. The voltage gain is more than unity for load resistance of more than 20 ohms.

Acknowledgements

The authors would like to thank the Indian National Academy of Engineering for funding the project through INAE-SERB, DST Abdul Kalam Technology Innovation National Fellowship, 2023. The authors would also like to thank all the staff of the Division of Extracorporeal Devices of the Department of Medical Devices Engineering for their support in developing and testing the method described in the paper.

References

[1]. Nair, S. S., Muniyandi, M., DS, N., CV, M., & Joseph, R. (2023). Charging Current Characteristics and Effect of Casing Material in Wireless Recharging of Active Implantable Medical Devices Using Transcutaneous Energy Transfer System. Progress in Electromagnetics Research M, 122.

[2]. Moore, J., Castellanos, S., Xu, S., Wood, B., Ren, H., & Tse, Z. T. H. (2019). Applications of wireless power transfer in medicine: State-of-the-art reviews. Annals of biomedical engineering, 47, 22-38.

[3]. Zhou, Y., Liu, C., & Huang, Y. (2020). Wireless power transfer for implanted medical application: A review. Energies, 13(11), 2837.

[4]. Campi, T., Cruciani, S., Feliziani, M., & Hirata, A. (2014, May). Wireless power transfer system applied to an active implantable medical device. In 2014 IEEE Wireless Power Transfer Conference (pp. 134-137). IEEE.

[5]. Puers, R., & Vandevoorde, G. (2001). Recent progress on transcutaneous energy transfer for total artificial heart systems. Artificial organs, 25(5), 400-405.

[6]. Kim, J. H., Hassan, N. U., Lee, S. J., Jung, Y. W., & Shin, S. U. (2022). A resonant current-mode wireless power transfer for implantable medical devices: an overview. Biomedical Engineering Letters, 12(3), 229-238.

[7]. Goldstein, D. J., Naftel, D., Holman, W., Bellumkonda, L., Pamboukian, S. V., Pagani, F. D., & Kirklin, J. (2012). Continuous-flow devices and percutaneous site infections: clinical outcomes. The Journal of heart and lung transplantation, 31(11), 1151-1157.

[8]. Schuder, J. C. (2002). Powering an artificial heart: birth of the inductively coupled-radio frequency system in 1960. Artificial organs, 26(11), 909-915.

[9]. RamRakhyani, A. K., Mirabbasi, S., & Chiao, M. (2010). Design and optimization of resonance-based efficient wireless power delivery systems for biomedical implants. IEEE transactions on biomedical circuits and systems, 5(1), 48-63.

[10]. Knecht, O., Bosshard, R., Kolar, J. W., & Starck, C. T. (2014, June). Optimization of transcutaneous energy transfer coils for high power medical applications. In 2014 IEEE 15th Workshop on Control and Modeling for Power Electronics (COMPEL) (pp. 1-10). IEEE.

[11]. Knecht, O., Bosshard, R., & Kolar, J. W. (2015). High-efficiency transcutaneous energy transfer for implantable mechanical heart support systems. IEEE Transactions on Power Electronics, 30(11), 6221-6236.

[12]. Jiang, C., Chau, K. T., Liu, C., & Lee, C. H. (2017). An overview of resonant circuits for wireless power transfer. Energies, 10(7), 894.

[13]. Sheng, H., Zhang, X., Liang, J., Shao, M., Xie, E., Yu, C., & Lan, W. (2021). Recent advances of energy solutions for implantable bioelectronics. Advanced Healthcare Materials, 10(17), 2100199.

[14]. Tamura, M., Murai, K., & Matsumoto, M. (2021, June). Design of disposable film-type capacitive wireless charging for implantable medical devices. In 2021 IEEE

International Research Journal on Advanced Engineering and Management
https://goldncloudpublications.com
https://doi.org/10.47392/IRJAEM.2024.0263
e ISSN: 2584-2854
Volume: 02
Issue: 05 May 2024
Page No: 1771-1777

MTT-S International Microwave Symposium (IMS) (pp. 58-61). IEEE.

[15]. Yi, X., Zheng, W., Cao, H., Wang, S., Feng, X., & Yang, Z. (2021). Wireless power transmission for implantable medical devices using focused ultrasound and a miniaturized 1-3 piezoelectric composite receiving transducer. IEEE Transactions on Ultrasonics, Ferroelectrics, and Frequency Control, 68(12), 3592-3598. Hached, S., Trigui, A., El Khalloufi, I., Sawan, M.,

[16]. Loutochin, O., & Corcos, J. (2014, April). A Bluetooth-based Low-Energy Qi-compliant battery charger for implantable medical devices. In 2014 IEEE International Symposium on Bioelectronics and Bioinformatics (IEEE ISBB 2014) (pp. 1-4). IEEE.

[17]. Mussivand, T., Miller, J. A., Santerre, P. J., Belanger, G., Rajagopalan, K. C., Hendry, P. J., ... & Keon, W. J. (1993). Transcutaneous energy transfers system performance evaluation. Artificial organs, 17(11), 940-947.

[18]. Rintoul, T. C., & Dolgin, A. (2004). Thoratec transcutaneous energy transformer system: a review and update. Asaio Journal, 50(4), 397-400.